Inorganic Chemistry

Communication

pubs.acs.org/IC

# Dynamic Metal–Organic Framework with Anion-Triggered Luminescence Modulation Behavior

Avishek Karmakar, Biplab Manna, Aamod V. Desai, Biplab Joarder, and Sujit K. Ghosh*

Department of Chemistry, Indian Institute of Science Education and Research, Dr. Homi Bhabha Road, Pashan, Pune 411021, India

Supporting Information

**ABSTRACT:** A three-dimensional cationic framework based on a flexible neutral nitrogen-donor ligand was synthesized and undergoes guest-driven structural dynamics in a reversible way. Size-selective anion-exchange and tunable luminescent behavior of the framework has been explored.

Porous coordination polymers or metal–organic frameworks (MOFs) with tunable properties have emerged as an exciting class of multifunctional materials because of their applications over a wide range.[1] In particular, "soft porous frameworks" have attracted much attention in recent years because of their highly ordered network along with structural flexibility.[2] They score over the conventional rigid porous frameworks in a way that they respond to a specific guest molecule and change their microcavities into those that match the shape and affinity of the incoming guest molecule. These materials undergo solid-state structural transformation when a guest molecule comes in or goes out of the framework. Such guest-responsive tailorable behavior along with enzyme-like specificity makes it a stimulus-responsive smart host material, thereby triggering a manifold increase in the host–guest interactions.[2,3] Combinations of a neutral flexible ligand and metal ions generally give rise to cationic frameworks.[4] These frameworks usually harbor solvents as guests in their porous cavities. Upon drying, these loosely trapped guests escape, thus leading to structural transformations.[5] These guest-driven structural transformations often find a way to build up a dynamic framework.[4b] In addition, these cationic MOFs have extra counteranions to neutralize the overall charge of the framework, which usually weakly coordinates to the metal ions or sometimes remains free in the framework lattice.[6] The incorporation of a $d^{10}$ metal ion in complexation with a nitrogen-donor ligand at room temperature often provides luminescent cationic frameworks.[7] Variation of the counteranions in a luminescent cationic framework by other foreign anions of different size, shape, and geometry may often regulate the framework functionalities.[8] Especially, the anion-switchable fluorescence of a luminescent cationic framework has been one of the most investigated topics in this regard because it finds very useful application such as chemical sensors and anion receptors, paving the way for a concoction of new materials.[4b,7,9] In spite of a lot of reports on dynamic frameworks, anion/guest-switchable fluorescence tuning of a MOF mixed with its inherent framework flexibility is not so common.[10,4b]

Herein, we present a three-dimensional (3D) cationic luminescent framework built from a newly designed nitrogen-donor ligand [(*E*)-*N*′-[1-(pyridin-4-yl)ethyidene]hydrazine carbohydrazide; Scheme S1 in the Supporting Information (SI)] with a flexible skeleton (Figure S1a in the SI) with multiple coordinating sites in combination with zinc(II). The framework shows guest-driven structural dynamics in a reversible way. The air-dried phase of the compound exhibits size-dependent anion-exchange behavior, and this is well demonstrated by single crystal-to-single crystal (SCSC) structural transformation experiments along with other spectroscopic techniques. The cationic framework shows interesting anion-responsive tunable luminescent behavior (Scheme 1).

**Scheme 1. Schematic Representation of a Guest- and Anion-Responsive Dynamic Framework**

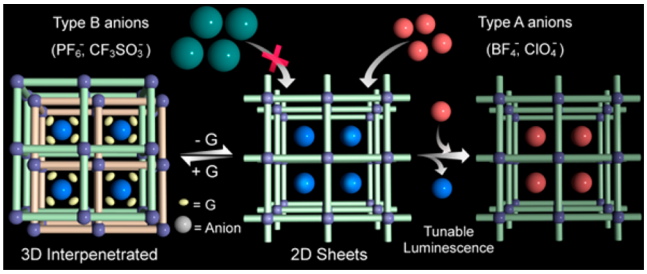


The combination of L (Scheme S1 in the SI) with zinc(II) in a solvent system of methanol/dichloromethane/chlorobenzene at room temperature yielded transparent block-shaped crystals of the compound $[\{Zn(L)_2\}(NO_3)_2{\cdot}xG]_n$ ( **1**′⊃$NO_3^-$; G is a disordered guest molecule). Single-crystal X-ray diffraction (SC-XRD) analysis of **1**′⊃$NO_3^-$ showed that it crystallized in a monoclinic system with space group *C*2/*c*. The asymmetric unit contains two ligands, one zinc(II) ion and two noncoordinated nitrate ($NO_3^-$) anions. Each zinc(II) ion displays distorted octahedral geometry with a $N_4O_2$ donor set from four ligands (Figure S1b in the SI). Two ligands bind in a bidentate fashion through amine nitrogen and carbonyl oxygen, and the other two connect the same zinc(II) node via pyridyl nitrogen, thus extending into a 3D structure, as shown in Figures S2 and S3 in the SI. 2-fold interpenetration creates large one-dimensional tubelike channels along the *b* axis, in which disordered solvent molecules and nitrate anions are located.

**Received:** June 20, 2014
**Published:** November 18, 2014

A noteworthy feature of the compound is that when $\mathbf{1}'\supset NO_3^-$ was kept out of the mother liquor at room temperature and air-dried for about 24 h, it shows a drastic structural change and is transformed to a new phase, which was evidenced from the time-dependent powder X-ray diffraction (PXRD) pattern (Figure S18 in the SI). PXRD patterns at various time intervals and in the presence of a small amount of mother liquor indicate that the structural integrity is initially maintained. However, after about 1−6 h, the PXRD pattern shows a drastic structural change and converts to a new phase, $\mathbf{1}\supset NO_3^-$, which demonstrates the dynamic nature of compound $\mathbf{1}'\supset NO_3^-$. Furthermore, when $\mathbf{1}\supset NO_3^-$ is reimmersed in the mother liquor, compound $\mathbf{1}\supset NO_3^-$ reverts back to compound $\mathbf{1}'\supset NO_3^-$, as shown by the PXRD pattern (Figure S19 in the SI), indicating the reversible nature of the framework. Because of the weak crystalline nature of $\mathbf{1}\supset NO_3^-$, the structure could not be obtained even after several attempts. Because $\mathbf{1}'\supset NO_3^-$ showed structural transformation at room temperature, we performed anion-exchange experiments with the air-stable phase $\mathbf{1}\supset NO_3^-$, which also contains the framework $NO_3^-$ [confirmed by IR and energy-dispersive X-ray (EDX) spectra; see the SI]. Anion-induced structural changes are observed when attempts are made to exchange $\mathbf{1}\supset NO_3^-$ with other anions (Figure 1). Anion-

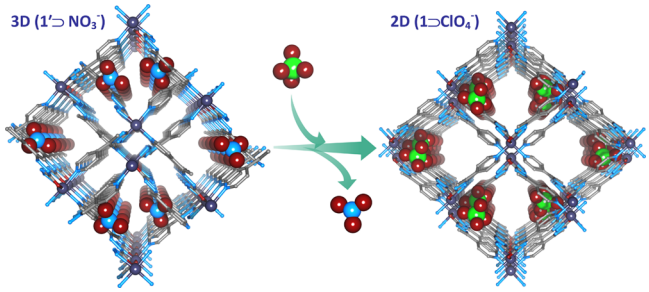


**Figure 1.** Perspective view of the solid-state structural transformation from $\mathbf{1}'\supset NO_3^-$ to $\mathbf{1}\supset ClO_4^-$ showing the overall packing of both phases.

exchange completion was monitored by dipping the crystals of $\mathbf{1}\supset NO_3^-$ in separate methanolic solutions of $NaClO_4$, $NaBF_4$, $KPF_6$, $KSbF_6$, and $NaCF_3SO_3$ and thereafter characterized by FT-IR spectra and CHNS data after about 4−5 days. FT-IR spectra of the anion-exchanged products show strong bands that are characteristic of the exchanged anions. For compound $\mathbf{1}\supset NO_3^-$ with $NO_3^-$ anions, inside the channels, a characteristic band at 1380 $cm^{-1}$ is observed as a result of the nitrate anion. However, the ligand (L) shows a characteristic band around the same region as that of the $NO_3^-$ anion due to C−C aromatic stretch (Figure S30 in the SI). Therefore, although the intensity of this band is unchanged in the exchanged products, new peaks at 1080 $cm^{-1}$ ($\mathbf{1}\supset ClO_4^-$) and 1034 $cm^{-1}$ ($\mathbf{1}\supset BF_4^-$) are observed in the respective exchanged compounds (Figure 2). For $PF_6^-$, $SbF_6^-$, and $CF_3SO_3^-$, because of larger size, these anions could not be exchanged and therefore show no characteristic peak in IR spectra (Figure S29 in the SI) even after 5−10 days. Selective anion exchange, i.e., separation of anions based on similar shape and size, is one of the intriguing aspects of such dynamic anion-exchange processes. In a typical experiment, crystals of $\mathbf{1}\supset NO_3^-$ are immersed in a methanolic solution of mixed anions ($BF_4^-$/$ClO_4^-$) having equimolar concentration (see the SI). Selective anion exchange by the framework was observed in which $NO_3^-$ was quantitatively exchanged with $BF_4^-$ (Figure S29 in the SI). Reversibility could not be attained when we tried to exchange

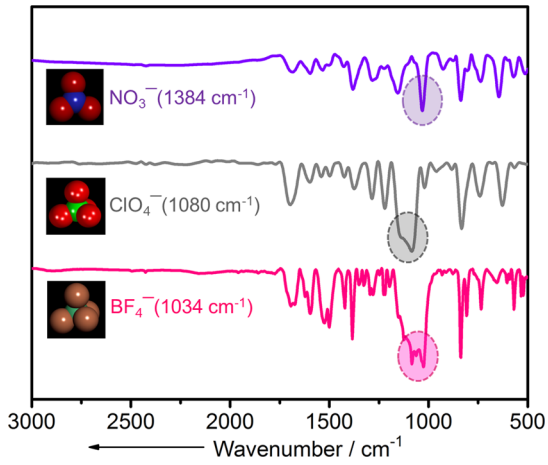


**Figure 2.** FT-IR spectra of $\mathbf{1}\supset NO_3^-$ and different anion-exchanged compounds showing highlighted bands for corresponding anions.

both $ClO_4^-$ and $BF_4^-$ with excess $NO_3^-$ because of the stronger hydrogen-bonding interaction of $ClO_4^-$ and $BF_4^-$ with the framework lattice (Figures S13 and S31 in the SI).

During the anion-exchange process, X-ray-quality single crystals were obtained for $\mathbf{1}\supset ClO_4^-$ and $\mathbf{1}\supset BF_4^-$, respectively. Single-crystal analysis of compound $\mathbf{1}\supset ClO_4^-$ and $\mathbf{1}\supset BF_4^-$ revealed that both compounds $[\{Zn(L)_2\}(ClO_4)_2\cdot xG]_n$ ($\mathbf{1}\supset ClO_4^-$) and $[\{Zn(L)_2\}(BF_4)_2\cdot xG\}]_n$ ($\mathbf{1}\supset BF_4^-$) crystallized in a monoclinic system and were isostructural. The asymmetric unit of compound $\mathbf{1}\supset ClO_4^-$ contains half of a zinc ion, one ligand, and one noncoordinated $ClO_4^-$ anion. The zinc(II) ion displays perfect octahedral geometry, with the $N_4O_2$ donor set having the same coordination environment as that in the case of $\mathbf{1}'\supset NO_3^-$, forming two-dimensional (2D) network. Interestingly, close examination of all of the structures revealed that during structural transformation the $L-Zn^{II}-L$ angle for the compounds is quite different from 106.22° ($\mathbf{1}'\supset NO_3^-$) compared to 112.17° ($\mathbf{1}\supset ClO_4^-$) and 66.49° ($\mathbf{1}\supset BF_4^-$; Figure S34 in the SI). This is probably due the cooperative effect of ligand flexibility and the loss of low-boiling solvents from the lattice voids, which leads to the drastic change in the overall network with Zn−N bond rearrangements, thereby resulting in the formation of these more stable 2D structures. Single-crystal structural analysis showed complete exchange of $NO_3^-$ in $\mathbf{1}\supset NO_3^-$ by incursive anions in the exchanged compounds, whereas the bulk powder FT-IR analysis and CHNS data revealed ∼98% exchange of the same. The PXRD patterns of compounds $\mathbf{1}\supset ClO_4^-$ and $\mathbf{1}\supset BF_4^-$ match exactly with their respective simulated patterns, and this proves the phase purity of the bulk sample (Figures S20 and S21 in the SI) after anion exchange. As observed, compound $\mathbf{1}'\supset NO_3^-$ upon air drying transforms to a stable phase ($\mathbf{1}\supset NO_3^-$), which thereby undergoes SCSC transformation after anion exchange to form structures $\mathbf{1}\supset ClO_4^-$ and $\mathbf{1}\supset BF_4^-$. More interestingly, the PXRD pattern of $\mathbf{1}\supset ClO_4^-$ is also quite similar to the experimental PXRD pattern of compound $\mathbf{1}\supset NO_3^-$, thereby indicating that compound $\mathbf{1}\supset NO_3^-$ probably is isostructural with $\mathbf{1}\supset ClO_4^-$ and $\mathbf{1}\supset BF_4^-$ (Figure S19 in the SI). Thermogravimetric analysis (TGA) of compounds $\mathbf{1}\supset NO_3^-$, $\mathbf{1}\supset ClO_4^-$, and $\mathbf{1}\supset BF_4^-$ demonstrates that the compounds were thermally stable up to ∼225 °C with an initial loss because of lattice solvent molecules (Figures S23−S25 and S26−S28 in the SI). Guest-inclusion behavior for compounds $\mathbf{1}\supset NO_3^-$, $\mathbf{1}\supset ClO_4^-$, and $\mathbf{1}\supset BF_4^-$ was examined by solvent sorption measurements at 298 K. The


dx.doi.org/10.1021/ic501477u | Inorg. Chem. 2014, 53, 12225−12227

ethanol sorption profile for compound $1\supset NO_3^-$ showed a typical hysteretic gate-opening nature ($P/P_0 = 0.78$) of dynamic frameworks and an uptake amount of about 152 mL $g^{-1}$ (6.82 mmol $g^{-1}$). For anion-exchanged compounds $1\supset ClO_4^-$ and $1\supset BF_4^-$, the uptake amounts are 135 mL $g^1$ (6.035 mmol $g^{-1}$) and 173 mL $g^{-1}$ (7.74 mmol $g^{-1}$) (Figure S33 in the SI) with similar sorption patterns. The difference is the sorption amount with similar sorption patterns is due to the differential interaction of guest with similar frameworks but containing anions of different shape, size, and electronic nature.

UV absorptions were measured in order to check the absorption profile for anion-exchanged compounds. Compound $1\supset NO_3^-$ and anion-exchanged compounds show similar nature in the absorption curves (Figure S35 in the SI). Also, solid-state emission spectra were investigated for powdered samples of L and desolvated compounds of both $1\supset NO_3^-$ and other anion-exchanged samples at room temperature.

Upon photoexcitation at 350−400 nm, L displays a weak fluorescence and, consequently, emission maxima at 440 nm. Compound $1\supset NO_3^-$ showed an intense broad band at 505 nm exhibiting a significant red shift compared to L. This can be attributed to $\pi^*-\pi$ intraligand transitions, metal-to-ligand charge transfer, or the effect of coordination of the ligand to the metal center. $1\supset ClO_4^-$ and $1\supset BF_4^-$ display broad peaks with intensity maxima at 442 and 497 nm, respectively. Both exchanged compounds showed a blue shift with respect to emission of $1\supset NO_3^-$ (Figure3). The emission intensity of exchanged

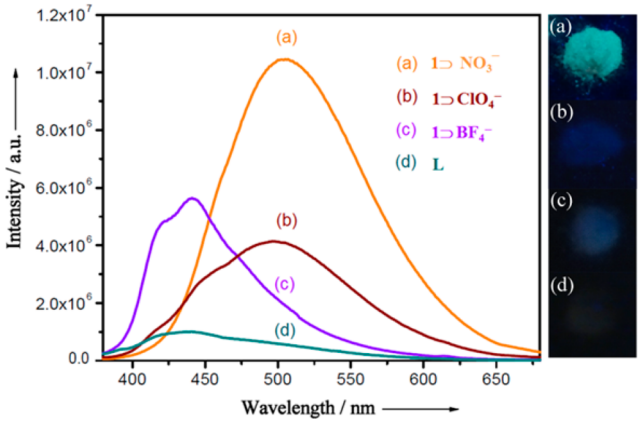


**Figure 3.** Solid-state emission spectra of $1\supset NO_3^-$, free-ligand, and anion-exchanged compounds (left) and optical micrographs of the same compounds under UV light (right).

compounds showed very drastic differences compared to$1\supset NO_3^-$, which may be due to the differential interaction of anions with the framework lattice. The quantum yields were measured for $1\supset NO_3^-$ and anion-exchanged compounds in the solid state at room temperature according to Bril and De Jager-Veenis.[11] The calculated quantum yield values of $1\supset NO_3^-$, $1\supset ClO_4^-$, and $1\supset BF_4^-$ are 0.873, 0.0583, and 0.0337, respectively, which supports the corresponding emission profiles of the respective compounds.

In conclusion, we have synthesized a luminescent cationic porous framework using a newly designed flexible chelating nitrogen-donor ligand. The framework showed guest-driven structural dynamics in a reversible manner. The framework contains free anions in its lattice voids. These anions can be exchanged easily by other anions of different shape and size. These anion-exchange experiments were well demonstrated by SCSC structural transformation and other spectroscopic techniques. Furthermore, selective anion-exchange results prove the affinity of the host framework toward anions of similar nature and can be an efficient system for ion separation. Also, anion-exchanged compounds show anion-dependent tunable luminescence and therefore have potential to develop as smart materials for chemical sensors, light-emitting devices, and other optoelectronic design strategies.

## ■ ASSOCIATED CONTENT

### Ⓢ Supporting Information

X-ray crystallographic data in CIF format, synthesis, FT-IR, TGA, and PXRD data, and X-ray tables. This material is available free of charge via the Internet at http://pubs.acs.org.

## ■ AUTHOR INFORMATION

### Corresponding Author

*E-mail: sghosh@iiserpune.ac.in. Phone: +91 20-2590-8076. Fax: +91-20-2590-8186.

### Author Contributions

The manuscript was written through contributions of all authors.

### Notes

The authors declare no competing financial interest.

## ■ ACKNOWLEDGMENTS

B.M and B.J are thankful to the CSIR for a research fellowship. We are thankful to IISER Pune and DST (Project GAP/DST/CHE-12-0083) for financial support.

## ■ REFERENCES

(1) (a) Zhou, H. C.; Long, J. R.; Yaghi, O. M. *Chem. Rev.* **2012**, *112*, 673−674. (b) Park, I. H.; Chanthapally, A.; Zhang, Z.; Lee, S. S.; Zaworotko, M. J.; Vittal, J. J. *Angew. Chem., Int. Ed.* **2014**, *53*, 414−419. (c) Das, M. C.; Bharadwaj, P. K. *J. Am. Chem. Soc.* **2009**, *131*, 10942−10949. (d) Ohba, M.; Yoneda, K.; Agustí, G.; Muñoz, M. C.; Gaspar, A. B.; Real, J. A.; Yamasaki, M.; Ando, H.; Nakao, Y.; Sakaki, S.; Kitagawa, S. *Angew. Chem., Int. Ed.* **2009**, *48*, 4767.

(2) (a) Horike, S.; Shimomura, S.; Kitagawa, S. *Nat. Chem.* **2009**, *1*, 695−704. (b) Schneemann, A.; Bon, V.; Schwedler, I.; Senkovska, I.; Kaskel, S.; Fischer, R. A. *Chem. Soc. Rev.* **2014**, *43*, 6062−6096.

(3) Kitayama, N. K.; Hijikata, Y.; Sato, H.; Matsuda, R.; Kubota, Y.; Takata, M.; Mizuno, M.; Uemura, T.; Kitagawa, S. *Nat. Mater.* **2011**, *10*, 787−793.

(4) (a) Wang, J. H.; Li, M.; Li, D. *Chem. Sci.* **2013**, *4*, 1793−1801. (b) Manna, B.; Chaudhari, A. K.; Joarder, B.; Karmakar, A.; Ghosh, S. K. *Angew. Chem., Int. Ed.* **2013**, *52*, 998−1002.

(5) (a) Biradha, K.; Fujita, M. *Angew. Chem., Int. Ed.* **2002**, *41*, 3392−3395. (b) Lun, D. J.; Waterhouse, G. I. N.; Telfer, S. G. *J. Am. Chem. Soc.* **2011**, *133*, 5806−5809.

(6) Li, X.; Xu, H.; Kong, F.; Wang, R. *Angew. Chem., Int. Ed.* **2013**, *52*, 13769−13773.

(7) Hou, S.; Liu, Q. K.; Ma, J. P.; Dong, Y. B. *Inorg. Chem.* **2013**, *52*, 3225−3235.

(8) (a) Maji, T. K.; Matsuda, R.; Kitagawa, S. *Nat. Mater.* **2007**, *6*, 142−148. (b) Ma, J. P.; Yu, Y.; Dong, Y. B. *Chem. Commun.* **2012**, *48*, 2946−2948.

(9) Chen, B.; Wang, L.; Zapata, F.; Qian, G.; Lobkovsky, E. B. *J. Am. Chem. Soc.* **2008**, *130*, 6718−6719.

(10) Takashima, Y.; Martinez, V. M.; Furukawa, S.; Kondo, M.; Shimomura, S.; Uehara, H.; Nakahama, M.; Sugimoto, K.; Kitagawa, S. *Nat. Commun.* **2011**, *2*, 168.

(11) Bril, A.; De Jager-Veenis, A. W. *J. Res. Natl. Bur. Stand., Sect. A* **1976**, *80A*, 401−407.